{jt1522, 02279861}, {aj922,02345687}

1. Data Preparation

Time Series Visualisation In the provided dataset containing sensory data of six different objects, namely $\{$*acryclic, black foam, car sponge, flour sack, kitchen sponge, steel vase*$\}$, two distinct subgroups were identified; the steel vase and acrylic objects which are hard and stiff constitute the *hard* group, and the *foamy spongy* objects and flour sack constitute the *soft group*, which are generally softer and compressible. The data from the BioTac sensor includes measurements of absolute fluid pressure, high frequency fluid vibrations, and rate of change of temperature. Additionally, the impedance of 19 electrodes was also measured. In choosing a suitable slice of data for further analysis, the *soft* and *hard* groups were scrutinised independently, before being compared. Figure 1 shows the sensory data profiles of all the objects, and a comparison between the *hard* objects and the kitchen sponge is shown in figure 10 in the appendix. In selecting a timestep, using the average over all trials of an object was found to be more useful than arbitrarily choosing a subset of trials on which to make a decision.

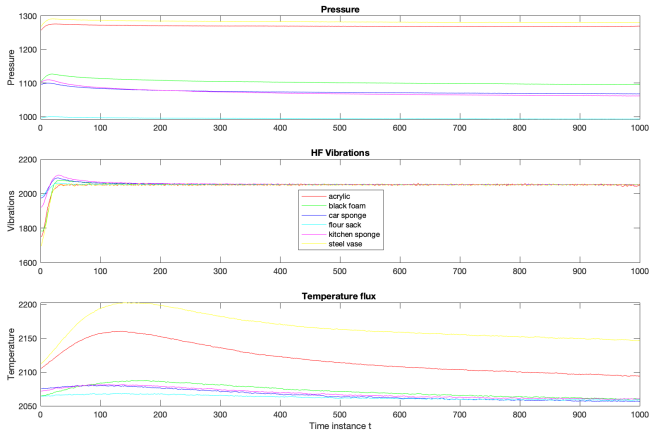

Figure 1: Pressure (P), vibration (V) and temperature flux (T) data of all six objects, averaged over ten experimental procedure trials for each object, plotted over time.

In both figures 1 and 10, we can see that the vibration values spike rapidly soon after the BioTac makes contact with the object, and then is damped quickly during the static hold procedure. Different objects exhibit different spike magnitudes and speed of dampening. Very quickly, the variance in the vibration data is greatly reduced, and with it, much of the information in the signal lost. Therefore, the search for an optimal slice of data for object discrimination was narrowed down to roughly between t=0 and t=100. At timestep zero, the gripper holding the BioTacs is open, closing very shortly after. Therefore the first 10 or so timesteps were excluded from consideration, allowing time for the characteristics of the different objects to express themselves in the signals.

In contrast to the *soft* objects, the *hard* objects result in significantly higher pressures during holding. This is to be expected, as the fluid inside the BioTac must be further compressed to grip harder objects as opposed to deformable, softer objects. The increased temperature flux exhibited by the acrylic and steel vase over the kitchen sponge demonstrates their characteristic high thermal conductivity, pulling heat quickly from the BioTac. The clear distinction between the *hard* and *soft* groups makes them easily distinguishable using these sensory modalities. Therefore, we searched for a timestep which would allow discrimination of within group classes. The maximum variance across the P, V and T data in each group was both observed and calculated. Since the dataset contains more 'soft' than 'hard' objects, the timestep corresponding to the maximum variance in the *soft* group was favoured. Accordingly, a timestep of **t=30** was selected, coinciding with the spike in the vibration data.

Data Visualisation Slicing the data set at t=30, we are left with a 180×1 vector which can be reshaped into a 60×3 matrix containing the P, V and T data in each column, for a total of 60 experimental procedure (EP) trials; ten for each of the six objects in the dataset. This data can be visualised in figure 2.

Notice the distance between the *hard* objects presented in red and yellow, and the *soft* objects which are slightly more clustered, yet contain enough variation to be distinguishable.

2. Principal Component Analysis

PCA of PVT Data To perform principal component analysis of the F0_PVT data, the data was structured into a 60 by 3 matrix, with P, V, and T as columns and observations as rows.

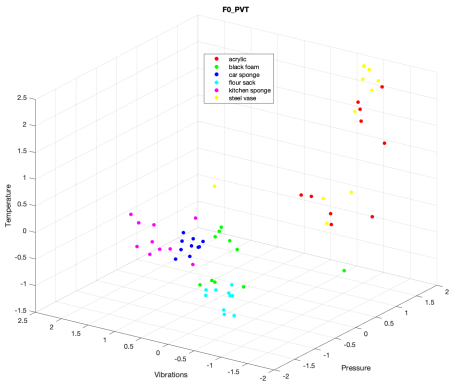

Figure 2: P, V, and T data for 10 EP trials per object, visualised in three dimensions.

Covariance Matrix of P, V, T data:

$$\begin{bmatrix} 1.0000 & -0.3892 & 0.9228 \\ -0.3892 & 1.0000 & -0.4914 \\ 0.9228 & -0.4914 & 1.0000 \end{bmatrix} \quad (1)$$

The Pressure and temperature data is highly positively correlated, and the pressure and vibration data are negatively correlated, suggesting there are redundancies in the data.

The eigenvectors of P,V,T data are shown as follows with each column being a separate vector. These vectors are the coefficients for each of the principal components.

$$\begin{bmatrix} 0.6206 & 0.3913 & -0.6795 \\ -0.4503 & 0.8873 & 0.0997 \\ 0.6419 & 0.2441 & 0.7269 \end{bmatrix} \quad (2)$$

The eigenvalues of the data are 2.2396, 0.6931, and 0.070. These represent the proportions of variance present in the data. The first eigenvector accounts for 74.6% of the variance, the second eigenvector accounts for 23.1%, and the third eigenvector accounts for 2.3% of the total variance.

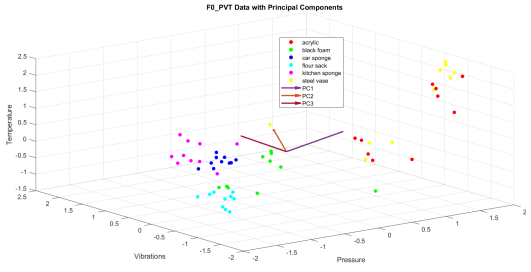

Figure 3: All P, V, T data at t = 30 standardized with the principal components of this data on the dataset

As one can see in figure 4, the two objects with the greatest variance along the first principal component are acrylic

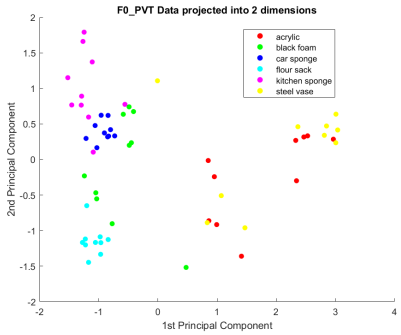

Figure 4: All P, V, T data at t = 30 projected into 2 dimensions with the axes as the first two principal components

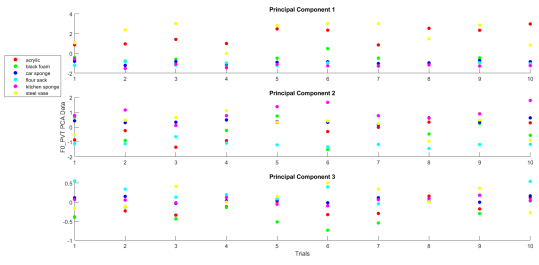

Figure 5: All P, V, T data at t = 30 distributed across each principal component

and the steel vase. These two objects also have considerable variance across the second principal components, and black foam varies the most across the first two principal component. Figure 5, shows the importance of PCA as the greatest range exists in principal component 1 across trials, and the lowest range is in principal component 3. This demonstrates the benefit of using PCA to project the majority of information in a dataset into fewer dimensions.

PCA of Electrode Data To analyze the electrode data, F0_Electrodes was structured into a 60 by 19 matrix with the columns as electrode readings and the rows as observations.

As seen in figure 11 the proportions of variance of the first three principal component are 65.7%, 30.5% and 2.0% respectively. These three components account for over 98% of the data which suggests only these would be needed for accurate object prediction. Figure 6 shows that the objects that have the greatest degree of overlap are acrylic and the steel vase, especially across the first two principal components. While the remaining objects across the first two principal components are clustered in their own regions.

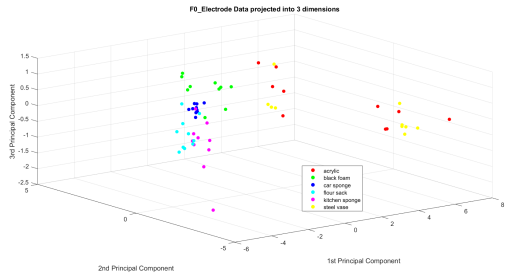

Figure 6: Visualisation of first three principal components of electrode data at t = 30

3. Linear Discriminant Analysis

To differentiate between the black foam and car sponge objects using P,V, and T data, Linear Discrimination Analysis (LDA) was performed first on each two dimensional combination of the data, and then on all three dimensions of the data at once. The results of the 2D LDA is shown in figure 7. Sub-figure 7d shows the projection of the P and T data onto the first linear discriminant (LD) line. Clearly, the data can be fully separated by the line $x = 0$, and indicates that pressure and temperature data contains the useful information for discrimination.

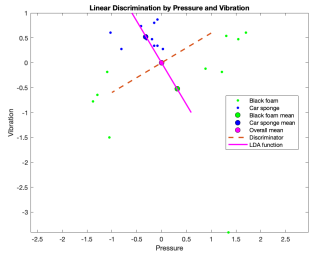

(a) LDA using P and V.

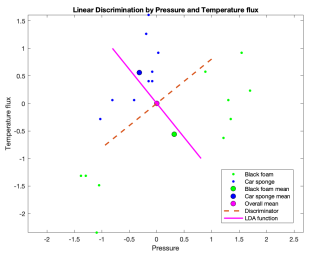

(b) LDA using P and T.

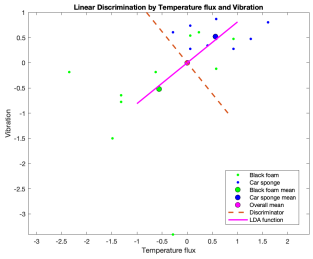

(c) LDA using V and T.

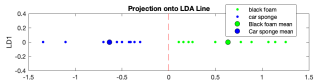

(d) P and T data (above) projected onto 1D LDA function.

Figure 7: Linear discrimination between the black foam (green) and car sponge (blue) objects using different combinations of P, V and T. The LDA function is shown in pink, and the discriminator in dashed red.

The magenta lines represent the first LD line, and the dashed red line is the discriminator between the two classes. The discriminators using P and V data, and V and T data respectively cannot fully separate the classes. The P and V discriminator in sub-figure 7a does a better job at separating the classes than the V and T discriminator in sub-figure 7c, as fewer examples lie on the incorrect side of the discriminator. This shows that we cannot use P and V data alone, or V and T data alone to fully separate the *soft* black foam and car sponge. However, P and T data alone contains sufficient information for full class separation in two dimensions. LDA was also performed using all sensory channels in three dimensions, shown in figure 8. The projection of the data onto the first two LD lines is shown in figure 12 in the appendix.

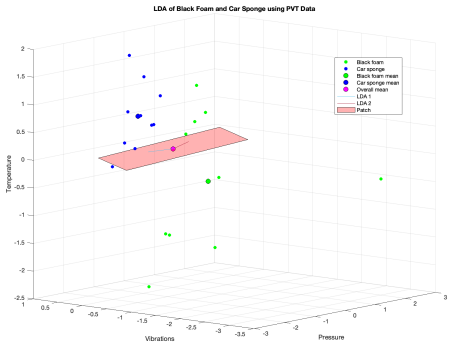

Figure 8: Linear Discrimination Analysis between the black foam and car sponge performed in three dimensions. The plane spanning the first two LDA lines is shown.

After projection, the data is fully separable in two dimensions, and exhibits a similar spatial distribution to the pressure and temperature plot presented in sub-figure 7b. This confirms that the P and T sensory channels are the best modalities to use for class separation. In figure 7b we can see on average, the car sponge sucks heat from the BioTac at a rate faster than the black foam. The black foam in the dataset [2] is seen to be very porous and has large air pockets within it. The car sponge is denser with smaller air pockets. Since air is a poor heat conductor and the black foam contains more air than the car sponge, heat is transferred from the BioTac to the black foam at a slower rate. The black foam shows a greater variation in pressure among trials, and on average requires a greater pressure to hold. This is possibly because the black foam contains more air and therefore more internal chamber-like structures, it can deform in slightly different ways between trials; some deformations requiring more pressure than others.

In a second experiment, LDA was performed on the P,V and T data of the acrylic and steel vase objects. We have shown that we can discriminate between two *soft* objects, therefore it would be of interest to see if we can discriminate between objects in the *hard* subgroup too. The results of the LDA are shown in figure 13 in the appendix.

Visualising the data projected onto the first LD line, it is

evident that the classes are not linearly separable. In this case, five out of a total 20 data points are misclassified, giving an accuracy of 75%. Since the timestep was chosen in a trade-off between intra- and inter- group variance, 75% accuracy seems an acceptable performance for intra-group classification considering inter-group accuracies of 100% can easily be achieved, and that classification within the *soft* subgroup can also be achieved with high accuracy. Indeed, even at a time instance optimal for classifying the acrylic from the steel vase, an accuracy of only 85% was achieved using LDA. Difficulty in classifying the acrylic and steel vase objects can be expected, since they exhibit extremely similar pressure and vibration profiles, with only limited information present in the their temperature profiles useful for discrimination. Moreover, 100% classification accuracy between the black foam and car sponge was not achieved using this new time instance, supporting our rationale for using the original **t=30**.

4. Clustering and Classification

Clustering K-Means clustering was performed on the P, V and T data across all objects, using a k-value of 6 and the euclidean distance metric. The resulting clusters are plotted in figure 9 below.

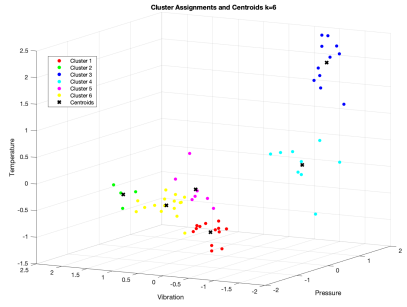

Figure 9: Clusters in the P, V and T data produced by MATLAB's K-Means algorithm with k=6 (equal to number of classes) and euclidean distance metric.

In the real data, analysed in the previous sections, the data points often overlap between classes. The classes output by the clustering algorithm, while potentially having similar centroids to the original classes in three dimensions, are all linearly separable. This is not realistic and most often not observed in real-life noisy data. The algorithm may have done a better job with some intuitive initialisation of the cluster centroids instead of random initialisation.
In a second clustering exercise, the manhattan distance was used in the K-Means algorithm. Using this distance metric, the algorithm produced seemingly more realistc data, with two classes exhibiting overlap not linearly separable in certain dimensions. This is possibly since the manhattan distance allows for clusters to contain points further away from their centroids since the distance of outliers is not exaggerated by a squared term as in euclidean distance.

Classification Bagging was applied to the electrode data that was processed with PCA. Only the first three principal components of the PCA data was used as this encompassed the majority of the variance in the electrode data. Six bags were chosen as these were the number of classes and this had the highest overall accuracy which was 91.67% as seen in the confusion matrix in figure 14.

The only incorrect classification was of the steel vase which was predicted to be acrylic. This is not too surprising as it was noted earlier that the two objects with greatest range along the first principal component were acrylic and the steel vase as seen in figure 6. Thinking qualitatively, these are the only two hard objects. The four other objects are soft and and as seen in 6 each of these objects has its own distribution across the first two principal components, while acrylic and the steel vase are notably similar. As soft objects are more compressible, it is understandable that these objects can have more identifiable compression signatures when being held while harder objects are tougher to differentiate. The application of PCA seems to have been helpful given a high accuracy was achieved and that the only objects misclassified were those that had the most similar PCA distributions.

5. Conclusions

PCA was effective in the identification of features containing the most information useful for distinguishing between objects. The features can then be used to classify the objects. This was performed successfully on the electrode data using bootstrap aggregation on the data projected onto the first three principal components, achieving an accuracy of 91.7%. By performing LDA on the P, V and T sensory data, we have managed to highlight which sensory modalities are most suited for classification. These are namely the pressure and temperature modalities which resulted in the highest classification accuracies, and would be preferable in a scenario where hardware or budget is limited. It has been shown that it is indeed possible to distinguish between certain objects using just touch data from a *hold* experimental procedure. Objects with similar physical properties proved difficult to distinguish when they exhibited very similar P and T profiles. An alternative data preparation approach would be to use time-series data rather than a single time step. One could divide the data into small time intervals and extract features corresponding to these intervals. Examples of approaches are RNN, LSTM, and CNN [1]. The benefits of this method is that it would identify temporal patterns in the data that are not present in a single time-step and thus could yield a higher accuracy. The main drawback is that this approach would be more computationally expensive and may be more difficult to interpret.

References

[1] W. Bottcher and et al. Object recognition for robotics from tactile time series data utilising different neural network architectures. In *2021 International Joint Conference on Neural Networks (IJCNN)*, 2021.

[2] V. Chu, I. McMahon, L. Riano, C. G. McDonald, Q. He, J. M. Perez-Tejada, M. Arrigo, N. Fitter, J. C. Nappo, T. Darrell, and K. J. Kuchenbecker. Using robotic exploratory procedures to learn the meaning of haptic adjectives. In *2013 IEEE International Conference on Robotics and Automation*, pages 3048–3055, 2013.

6. Appendix

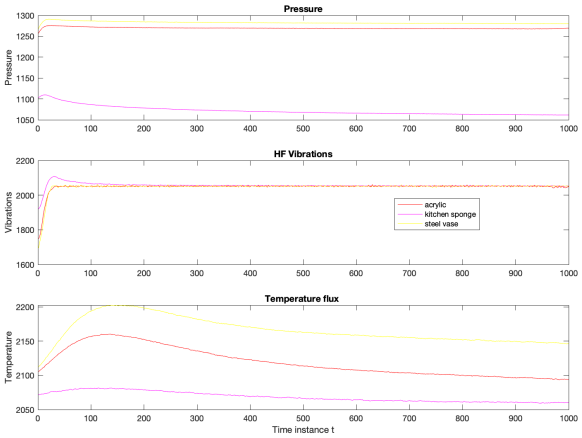

Figure 10: P, V and T sensory data for the *hard* objects, and the kitchen sponge for comparison, averaged over ten experimental procedure trials for each object.

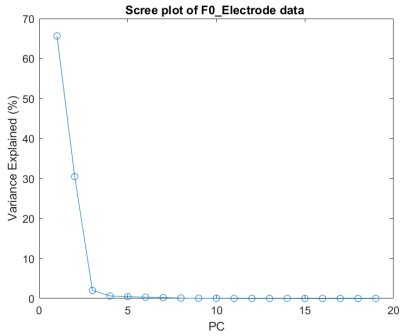

Figure 11: Scree plot of PCA of electrode data at t = 30

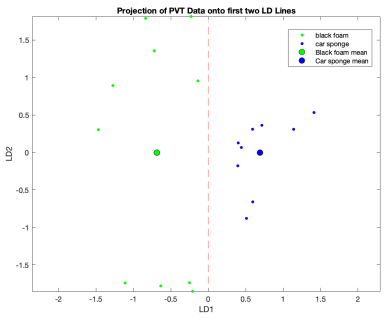

Figure 12: Three dimensional PVT data projected onto the first two LDA lines and plotted in two dimensions. The red dashed line shows the classification boundary.

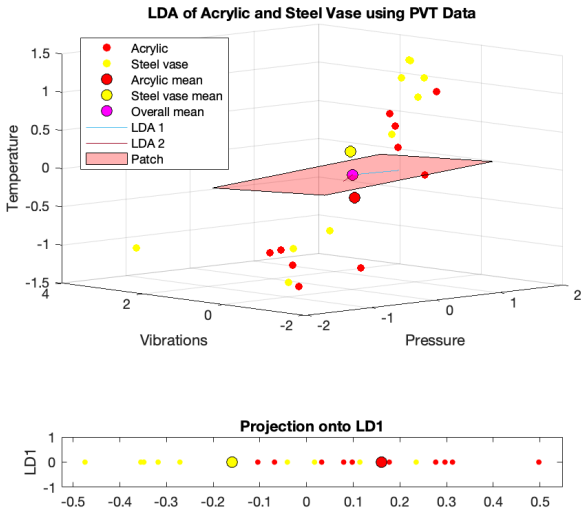

Figure 13: Linear Discrimination Analysis applied to the PVT data of the acrylic and steel vase objects. The projection of the data onto the first LDA line is shown. Apologies for difficult yellow color.

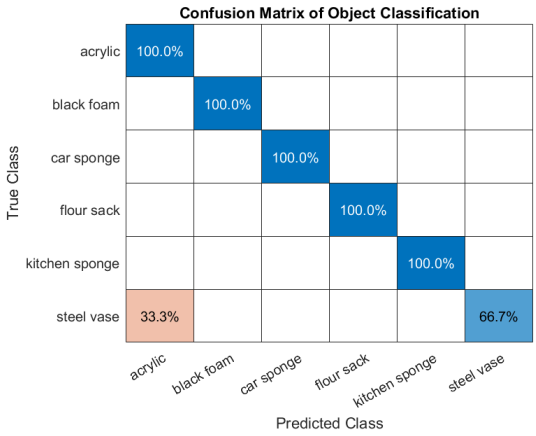

Figure 14: Confusion matrix of classification algorithm with 6 bags

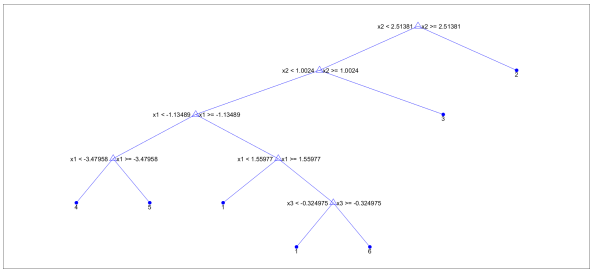

Figure 15: First decision tree generated by the classification algorithm

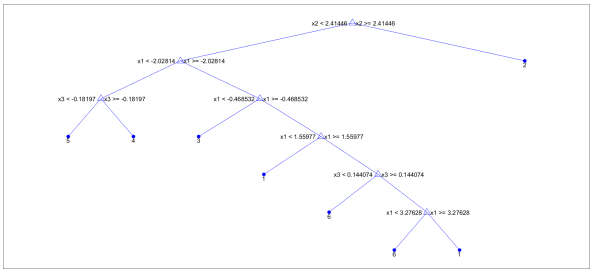

Figure 16: Fourth decision tree generated by the classification algorithm